



A Comprehensive Investigation of Coastal and Shelf Sediment Sources in the South Sea of Korea: A Marginal Sea of the Northwestern Pacific

Dhongil Lim¹ · Yeong-Gil Cho² · Dohyun Jeong¹ · Jihun Kim¹ · Zhaokai Xu³ · Taesoo Chang⁴

Received: 18 June 2023 / Revised: 25 August 2023 / Accepted: 30 August 2023 / Published online: 6 October 2023

© The Author(s), under exclusive licence to Korea Institute of Ocean Science & Technology (KIOST) and the Korean Society of Oceanography (KSO) and Springer Nature B.V. 2023

Abstract

To identify and quantify the sediment sources in the South Sea of Korea, a marginal sea of the northwestern Pacific, we analyzed a comprehensive aluminum–magnesium dataset comprising 121 surface sediment samples and two sediment cores. The findings demonstrate pronounced spatial variation in sediment sources, with Korean river sediments dominating in embayment bays and Chinese river sediments prevailing in the shelf area. In the coastal zone, Korean river sediments account for over 60–70%, but their proportion decreased to 10–20% in the shelf zone. This reveals that most of the sediments from Korean rivers are mainly confined to the coastal embayments, with limited transport to the shelf area. Notably, the central South Sea mud (CSSM) deposits are primarily governed by the sediment influx from Chinese rivers (CR), rather than the Seomjin River discharge. The prevalence of CR-sourced sediments in the shelf region is closely linked to the Tsushima Warm Current and Cheju Warm Current, transporting sediments from the East China Sea shelf northwards and the southwestern Korean coastal zone eastwards, respectively. This driving mechanism for the widespread deposition of CR sediments is further supported by an abrupt shift from KR to CR dominance in sediment sources around 8 kyr BP, coinciding with the establishment of the modern current systems in the northwestern Pacific marginal seas. Our study provides a new perspective on the source-to-sink pathways, particularly of Chinese river sediments, in the formation of the Korean coastal mud deposits.

Keywords Sediment provenance · Quantification · Mud depositions · Kuroshio Current · South Sea of Korea

1 Introduction

Deciphering sediment provenance and distribution pathways in marginal seas that encompass extensive river systems is pivotal for comprehending historical variations in paleoceanography and paleoclimate (Milliman and Meade 1983; Allen 2017; Zhao et al. 2018). In view of this, the sediment

source-to-sink pathways and the associated deposition processes in the Yellow Sea and the northern East China Sea (YECS), which are the epitome of epicontinental shelves in the northwestern Pacific marginal sea, have been rigorously conducted over recent decades (e.g., Park and Khim 1992; Cho et al. 1999, 2015; Yang et al. 2003; Yang and Youn 2007; Lim et al. 2020 and references therein). Remarkably, this body of research has zeroed in on the distinct mud patch deposits found in the YECS shelf (Fig. 1a), yielding valuable insights into the evolution of oceanic circulation systems and the complex interactions between land and ocean, often associated with climate shifts (Li et al. 2014; Hu et al. 2014a, b; Wang et al. 2014; Lim et al. 2015a and references therein). Moreover, these source-to-sink studies have uncovered the evolving influences of the Huanghe and Changjiang rivers in the formation of shelf mud deposits (Hu et al. 2014b; Dou et al. 2015; Lim et al. 2015a; Koo and Cho 2020), as well as the intricate mechanisms behind their formation, including the current systems of gyres and/or upwellings (Hu 1984; Shi et al. 2003; Bian et al. 2013; Wang et al. 2014).

✉ Dongil Lim
oceanlim@kiost.ac.kr

¹ South Sea Research Institute, Korea Institute of Ocean Science and Technology, Geoje 53201, Republic of Korea

² Department of Fisheries and Marine Resources, Mokpo National University, Mokpo 58554, Republic of Korea

³ CAS Key Laboratory of Marine Geology and Environment, Institute of Oceanology, Chinese Academy of Sciences, Qingdao 266071, China

⁴ Department of Geological and Environmental Sciences, Chonnam National University, Gwangju 61186, Republic of Korea

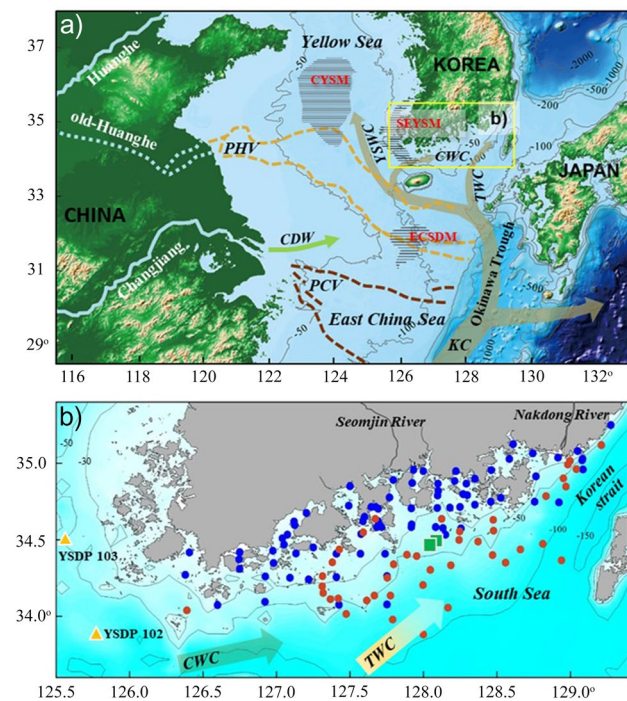


Fig. 1 **a** A map showing the study area including Kuroshio Current systems and paleo-river valleys. Hatched areas indicate the mud deposits. The paleo-river valleys (PCV and PHV) are modified from Hsiung and Saito (2017), Dou et al. (2016), Wang et al. (2015) and Yoo et al. (2016), respectively. **b** Sampling sites of the surface ($n=121$) and two core sediment samples for the study. Blue (this study) and red (Data from Cho 1994) dots: surface sediments, squares: two sediment cores (16PCT-GC01 and 16PCT-GC03, Data from Lee et al. 2019). KC Kuroshio Current, YSWC Yellow Sea Warm Current, TWC Tsushima Warm Current, CWC Cheju Warm Current, CDW Changjiang Diluted Water plume, CYSM Central Yellow Sea Mud, SEYSM Southeastern Yellow Sea Mud (or Hulsan Mud Belt, HMB), ECSDM East China Sea Distal Mud (or Southwestern Cheju Island Mud, SWCIM), PHV paleo-Huanghe valley, PCV paleo-Changjiang valley

Another intriguing revelation from source-to-sink investigations is the identification of sediments originated from Chinese rivers (CR) within the Korean coastal deposits. An earlier study on probing sediment sources highlighted a discrepancy between the total sediment budget and sediment contributions from Korean rivers (KR) within Korean coastal zones, hinting at the presence of supplementary sediment influx (Park et al. 2000; Lim et al. 2007). Subsequent studies employing clay mineral and elemental proxies reinforced the notion that these additional sediments primarily stemmed from the Changjiang and/or the Huanghe (e.g., Cho et al. 2015; Um et al. 2015; Kwak et al. 2016; Lim et al. 2013, 2020). In particular, these Korean coastal mud deposits displayed elevated contents of smectite and some elements (e.g., iron, magnesium, and heavy rare earth elements) which are characteristic of CR sediments. This finding implies a considerable inflow of fine-grained sediments

originating from Chinese rivers to the Korean coastal zones, particularly since around 6–8 kyr BP (Lim et al. 2020).

Despite the breadth of sediment source-to-sink research, dispersal patterns and quantities of sediments emanating from Chinese rivers remain contested topics, particularly in regard to the South Sea shelf of Korea, characterized by extensive mud deposits (Bae et al. 2014; Um et al. 2017; Kim et al. 2019; Lee, et al. 2019, 2023). The prevailing view has been that fine-grained sediments in the South Sea, especially within the inner shelf region, predominantly originate from Korean rivers, with the Seomjin and Nakdong Rivers being the major contributors (Fig. 1b). Nevertheless, the spatial extent of sediment dispersion from Korean rivers has not been definitively ascertained. Recently, Um et al. (2017) posited that sediments from Chinese rivers might have partially contributed to the formation of the thick mud deposit on the inner shelf of the central South Sea, known as the Central South Sea Mud (CSSM). However, this ‘multi origin’ hypothesis regarding the CSSM has yet to achieve consensus due to the scarcity of compelling evidence. Furthermore, the precise extent of CR source contributions to the South Sea shelf region, including the CSSM, remains to be clarified.

Various clay mineralogical and elemental proxies for discerning sediment sources in YECS mud deposits have been developed (e.g., Yang et al. 2003 and references therein; Xu et al. 2009; Lim et al. 2014, 2015a, b; Dou et al. 2015; Koo et al. 2018; Jung et al. 2021). Among these, alkaline earth elements, such as magnesium (Mg) and iron (Fe), have been widely acknowledged as reliable elemental markers for distinguishing different sources of fine-grained sediments in the YECS, as they exhibit distinct linear regression trends between groups of KR and CR sediments in correlation with aluminum (Al) (Lim et al. 2006a, 2013; Koo et al. 2018). Recently, an innovated approach for source quantification based on the advanced Al–Mg regression model was proposed, and this has been instrumental in achieving quantitative estimations of sediment source contributions (Lim et al. 2020). This methodology holds promise for more decisive sediment source discrimination in the South Sea of Korea, and for deepening our comprehension of sediment source-to-sink dynamics in the northwestern marginal seas.

In this study, our objectives are to distinguish and quantify the contributions of sediment sources from Chinese rivers (Changjiang and Huanghe) in the South Sea of Korea through the analysis elemental compositions of fine-grained sediments (with a mean grain size $> 4\phi$), with particular emphasis on Al and Mg data. The relative contributions of each source for the samples were calculated using the Al–Mg regression method as outlined by Lim et al. (2006a, 2020). We collected a total of 79 surface sediment samples from the coastal and shelf regions of the South Sea of Korea (Fig. 1b). To gain a more encompassing portrayal of the

spatial–temporal variations in sediment sources across the entire South Sea region, we also compiled and assessed data from prior studies. This approach enables us to capture and analyze nuanced information on sediment sources across the South Sea, thereby providing a comprehensive perspective on sediment dynamics within the region.

2 Regional Setting

The South Sea of Korea, situated at the northern extremity of the East China Sea, is bordered to the north by the numerous postglacial embayments and small islands, constituting a quintessential ria-type coast (Fig. 1a). The bathymetry is generally parallel to the coastline and extend to the E–W direction on the western part of the sea but turns to the NE–SW direction on the eastern part. The sediments are mostly composed of the modern fine sediments on the inner shelf and sand deposits on the outer shelf (Chough et al. 2000). Notably, the central area of the sea is distinguished by presence of the thick Holocene shelf mud deposits (i.e., CSSM) up to 20–30 m, which have accumulated since the last glacial maximum concurrent with the rise in sea levels (Park et al. 1996). The Seomjin and the Nakdong Rivers, the largest rivers flowing into the South Sea, contribute approximately 0.8×10^6 ton year⁻¹ and $4.6\text{--}10 \times 10^6$ ton year⁻¹, respectively (Lim et al. 2007 and references therein), to the coastal and inner shelf zones of the sea. The hydrodynamic conditions in the sea are primarily influenced by the northeastward Tsushima Warm Current (TWC), a branch of Kuroshio Current, and the coastal current in conjunction with Cheju Warm Current (CWC) which courses eastward along the southern coastline. Given these geographic and oceanographic characteristics, a reconstruction of the spatial and temporal variations in sediment sources in the South Sea may provide valuable insights into the dispersion limits of KR and/or CR sediments, as well as the evolution of TWC system over time.

3 Materials and Methods

Grain size analysis for surface sediments was performed using a standard dry-sieving technique for sand-sized fractions (> 63 μm), and a pipette method for mud fractions (silt- and clay-sized fractions; < 63 μm) after the removal of calcium carbonate and organic compounds. Textural parameters were calculated using the graphic method based on the weight percentages of each phi fraction (Ingram 1971). For the elemental contents (i.e., Al and Mg) of bulk sediments, each powdered sediment sample was fused with lithium meta-borate (LiBO_2) flux and the molten beads were subsequently poured into a volume of dilute nitric acid and

agitated until dissolved. The resultant solutions were analyzed using a Thermo iCAP 6500 radial inductively coupled plasma optical emission spectrometer. Standard reference material (MAG-1) was analyzed alongside a batch of sediment samples and the relative deviations between measured and certified values were found to be less than 5%. Analytical results, including previously reported data, are presented in Table 1.

In this study, the quantification of sediment sources is based on the Al–Mg regression model as proposed by Lim et al. (2006a, 2020). Briefly, the relative contributions of each sample were computed by calculating perpendicular distances between the position of a sediment sample on a scatter plot and each of the Al–Mg linear regression lines corresponding to KR and CR sediment groups (Fig. 2a). Specifically, the coordinates of the intersection point of the two regression lines representing KR and CR sediments were shifted to serve as the origin (0, 0), as the lines were not parallel (for further details, see Lim et al. 2006a); concurrently, the Al and Mg contents of all sediment samples from the study area were adjusted in accordance with the transformed origin. This correction essentially normalizes the bulk contents of the elements, accounting for variations in grain size, thereby refining sediment geochemistry.

In this study, a new Al–Mg linear regression line for the Korean river source was generated based on the combined data of the western Korean rivers (Lim et al. 2020) and the Seomjin River (Fig. 2a). This comprehensive dataset allowed more robust analysis and accurate estimation of source contributions for the sediments in the South Sea of Korea. The Al and Mg data of the Seomjin River are from fine surface sediments (Nam 2016) and short push-core sediments from the lower reaches of the river (Lim, personal communication). To ensure robust data collection and interpretation, furthermore, data from previous studies, including 42 surface sediment samples (Cho 1994) and two sediment core (Lee et al. 2019), were integrated with the newly acquired data (refer to Fig. 1b for sample sites).

4 Results and Discussion

In this study, we examined grain sizes and Al and Mg contents of 121 surface sediments and two sediment cores, incorporating previous data, to deepen our understanding of sediment sources, with a particular emphasis on their quantitative contributions in the entire South Sea shelf. The surface sediments mainly comprise fine-grained muds, with mean grain sizes ranging from 4.32 to 9.70 ϕ (average: $7.53 \pm 1.33 \phi$) (Fig. 3a). The content of mud (silt + clay) exceeds 80% (range: 33 to 100%) in most of the sediments, whereas the sand content is generally below 10% (Fig. 3b). The Al_2O_3 and MgO contents in surface and core sediments range from

Table 1 Mean grain size (Mz), contents of mud, Al₂O₃, and MgO for all surface sediment samples. Data of sample code 80 to 121 was from Cho (1994)

Sample Code	Latitude (°N)	Longitude (°E)	Mz (φ)	Mud (%)	Al ₂ O ₃ (%)	MgO (%)	Sample Code	Latitude (°N)	Longitude (°E)	Mz (phi)	Mud (%)	Al ₂ O ₃ (%)	MgO (%)
1	34.7160	127.6439	7.42	100	16.38	2.52	62	34.4200	126.7500	-	-	16.28	2.32
2	34.7158	127.6746	8.85	99	16.53	2.50	63	34.3100	126.7500	-	-	17.89	2.63
3	34.5836	127.6822	7.40	99	15.62	2.37	64	34.6200	127.1200	-	-	14.83	2.18
4	34.5834	127.7146	7.75	96	15.55	2.35	65	34.5100	127.0400	-	-	14.36	2.18
5	34.5766	128.1333	-	-	15.90	2.50	66	34.4700	127.0500	-	-	14.75	2.38
6	34.5333	128.1500	-	-	14.90	2.20	67	34.4500	127.2500	-	-	12.49	1.78
7	34.7048	127.6909	8.05	99	15.51	2.65	68	34.8500	127.5000	-	-	17.72	2.25
8	34.6235	127.6913	7.56	97	14.65	2.29	69	34.6000	127.9200	-	-	16.58	2.50
9	34.6219	127.5894	8.22	99	15.69	2.67	70	34.6500	127.6000	-	-	14.81	2.48
10	34.7230	127.4922	7.64	98	15.04	2.42	71	34.7100	128.1800	-	-	15.91	2.63
11	34.5377	127.5747	7.22	98	13.19	1.93	72	34.8200	128.1000	-	-	23.26	2.97
12	34.4096	127.5712	6.83	99	12.33	1.73	73	34.9500	128.0000	-	-	21.23	2.42
13	34.4100	127.7401	7.48	98	14.08	2.16	74	34.7300	128.3500	-	-	18.40	2.98
14	34.2637	127.7522	8.64	99	16.20	2.90	75	34.8000	128.2700	-	-	19.72	3.22
15	34.0792	127.7522	8.59	100	15.19	2.67	76	34.9000	128.3500	-	-	19.34	3.18
16	34.0759	127.4251	8.11	99	13.80	2.43	77	34.9500	128.2200	-	-	16.32	2.65
17	34.2567	127.4077	6.95	94	13.10	1.92	78	35.0200	129.0800	-	-	13.06	2.15
18	34.4106	127.4084	5.86	74	11.40	1.49	79	35.0800	129.0500	-	-	17.36	2.75
19	34.2408	127.2184	7.50	98	14.00	2.25	80	35.1200	129.2117	8.80	95	15.32	2.38
20	34.2529	127.0915	5.98	77	12.61	1.87	81	34.7867	128.8333	7.60	74	13.70	2.32
21	34.4107	127.1333	7.42	97	13.28	2.14	82	34.4900	128.3717	9.10	92	15.77	2.87
22	34.5352	127.0741	7.83	97	14.73	2.36	83	34.3517	128.5583	7.00	70	12.81	2.32
23	34.5971	127.1239	7.35	93	14.06	2.22	84	34.3333	128.1867	5.60	46	11.96	1.92
24	34.6755	127.2040	6.80	97	14.03	2.02	85	34.2050	127.9967	8.20	85	14.33	2.47
25	34.4288	126.9748	7.73	98	14.89	2.32	86	34.0567	128.1667	5.20	50	13.32	2.37
26	34.2602	126.9241	5.22	47	11.58	1.79	87	33.8833	128.0000	5.00	43	8.77	1.68
27	34.0949	126.9213	4.39	34	8.69	1.27	88	34.3667	128.9400	5.30	39	10.40	1.82
28	34.3738	126.7442	7.91	91	16.08	2.22	89	34.4750	128.8117	7.70	75	11.85	2.25
29	34.0732	126.5997	4.59	44	9.15	1.58	90	34.4383	128.6600	6.90	58	13.28	2.32
30	34.2716	126.3802	4.35	55	10.78	1.83	91	34.2533	127.7533	9.30	99	16.28	2.82
31	34.4183	126.4064	7.78	98	15.26	2.41	92	33.9800	127.7900	7.40	69	10.57	1.98
32	35.2503	129.2747	7.69	91	14.69	2.36	93	34.1367	127.6667	9.70	99	14.74	2.83
33	35.1205	129.2113	5.75	62	11.53	1.95	94	34.1167	127.4200	8.70	97	14.06	2.27
34	35.0302	129.0835	8.18	96	15.25	2.49	95	34.0167	127.4750	9.10	92	14.26	2.62
35	34.9596	129.0849	6.72	76	13.50	2.26	96	34.0400	126.3907	5.30	46	9.66	1.77
36	34.7461	128.9223	4.32	38	8.59	1.34	97	34.6383	127.6717	7.20	91	13.26	2.07

Table 1 (continued)

Sample Code	Latitude (°N)	Longitude (°E)	Mz (φ)	Mud (%)	Al ₂ O ₃ (%)	MgO (%)	Sample Code	Latitude (°N)	Longitude (°E)	Mz (φ)	Mud (%)	Al ₂ O ₃ (%)	MgO (%)
37	34.7498	128.7567	4.69	37	11.12	1.66	98	34.5483	127.5917	7.30	98	13.55	2.03
38	34.9149	128.7657	8.69	98	15.62	2.78	99	34.4367	127.4267	6.60	91	12.64	1.68
39	35.0389	128.9163	6.18	62	15.89	1.79	100	34.3533	127.3800	6.50	77	13.06	1.90
40	35.0649	128.7431	6.43	90	16.24	2.42	101	34.2633	127.3133	7.10	86	13.23	2.02
41	35.1268	128.6107	7.84	89	18.11	2.29	102	34.1533	127.3167	7.30	84	14.19	2.38
42	35.0302	128.5836	8.66	99	17.17	2.67	103	34.9633	129.0400	8.90	99	15.68	2.45
43	34.9559	128.4616	8.88	99	16.08	2.57	104	35.0167	128.9967	7.90	91	15.74	2.07
44	34.7486	128.4572	7.90	85	14.20	2.68	105	34.9933	128.9817	6.50	76	16.72	1.83
45	34.7759	128.5264	8.45	94	15.30	2.89	106	34.9017	128.9533	8.20	98	15.19	2.38
46	34.5746	128.2560	8.45	95	15.49	2.83	107	34.8483	128.9700	8.90	98	14.55	2.60
47	34.7151	128.2501	8.58	98	15.78	2.85	108	34.6317	128.4750	5.50	73	10.45	1.52
48	34.7918	128.2975	8.75	97	16.17	2.94	109	34.5600	128.4767	9.20	96	15.38	2.82
49	34.8686	128.2929	8.77	99	16.33	3.02	110	34.6383	128.1250	8.90	99	15.51	2.70
50	34.8844	128.2118	8.29	94	16.28	2.85	111	34.5567	128.2467	9.10	96	15.11	2.67
51	34.8673	128.0995	8.28	95	16.54	2.63	112	34.5000	128.2417	9.20	99	14.96	2.70
52	34.7894	128.0965	8.71	98	16.54	2.86	113	34.4000	128.4700	8.90	96	14.25	2.52
53	34.7089	128.0949	8.20	97	15.65	2.66	114	34.3050	128.0467	9.20	100	14.57	2.58
54	34.5840	128.0835	8.42	98	15.60	2.74	115	34.3950	127.9533	8.80	99	15.11	2.62
55	34.5834	127.9174	7.74	98	14.49	2.35	116	34.4033	127.8867	8.80	100	15.45	2.62
56	34.7061	127.9183	7.60	96	14.97	2.43	117	34.3417	127.7967	9.10	100	15.19	2.63
57	34.7767	127.7689	6.96	87	15.93	2.27	118	34.1367	127.7750	8.90	100	14.38	2.58
58	34.8913	127.7957	4.66	38	15.02	1.64	119	34.1033	127.6150	7.30	99	14.74	2.57
59	34.9586	127.9335	8.43	98	16.94	2.42	120	34.1133	127.3667	8.40	99	13.94	2.40
60	34.8714	127.9246	6.12	78	17.75	2.57	121	34.1967	127.3100	7.80	94	12.68	1.87
61	34.3500	126.9800	—	—	15.60	2.38							

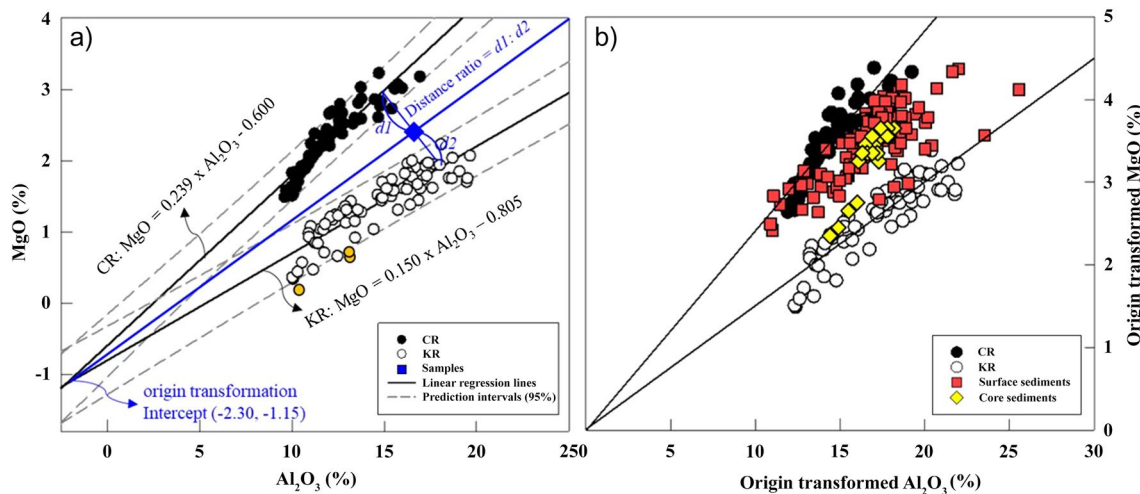


Fig. 2 a Al–Mg linear regression model for quantitative source estimate of the Korean rivers (KR) and Chinese rivers (CR) (modified from Lim et al. 2020). For the KR regression line, the Seomjin River data ($N=22$) are newly added to previous dataset from the western Korean rivers ($N=55$, Lim et al. 2020). The Seomjin River data are from fine surface sediments ($N=12$, Nam 2016) and short push-core sediments from the lower reaches of the river basin ($N=10$, Lim, per-

sonal communication). Some outliers (filled circles) in the KR sediments are removed. For more explanation of this model, the reader is referred to the text. b Origin-transformed Al–Mg discriminant diagram for sediment samples from the study area. Note that all of the sediment samples are distributed between the KR and CR sources, suggesting that they are a mixture of both sources

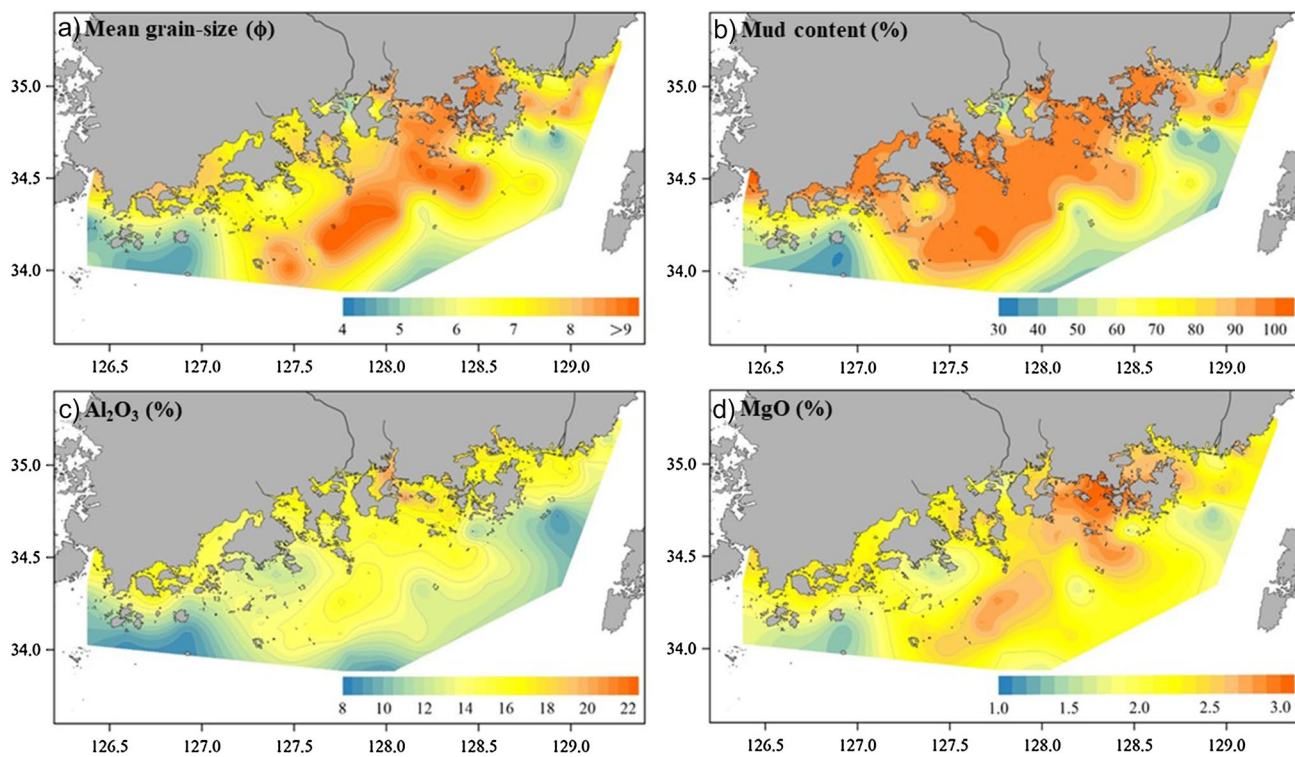


Fig. 3 Spatial distributions of a mean grain size, b mud content, c Al_2O_3 , and d MgO contents of sediments

8.59 to 23.26% (average: $14.69 \pm 2.33\%$) and 1.27 to 3.22% (average: 2.35 ± 0.40), respectively (Fig. 3c, d). Notably,

their spatial variations are aligned with the mean grain size distribution.

Mg has been established as a definitive tracer for identifying sediment provenance in the YECS. The Al–Mg correlation plot distinctly reveals different linear regression lines for the KR and CR sediments (Fig. 2a), signifying a marked difference in Mg content between the two groups, despite similarities in grain size. This divergence in Mg content is ascribed to the contrasting source rocks in each river basin. Sediments from Korean rivers are predominantly characterized by higher contents of quartz and potassium feldspar, whereas sediments from Chinese rivers contain a greater proportion of mafic rocks, including an abundance of ferromagnesian minerals and plagioclase feldspars (Lim et al. 2014, 2015b). Interestingly, in the Al–Mg discrimination plot, surface sediments from the study area are distributed between the KR and CR sources and exhibit distinct linear regression trends that deviate from those of the KR and CR sediments (Fig. 2b), suggesting that the surface sediments comprise a combination of both sources. This observation enables estimation of the relative contributions from each source by measuring the perpendicular distances between the position of a sediment sample and each of the KR and CR linear regression lines (Fig. 2a).

Our quantitative source estimates across the South Sea region unambiguously demonstrate a spatial demarcation between contributions from the KR and CR sources (Fig. 4). Importantly, the spatial variation in sediment source is gradual from the coastal dominated by the Korean river source to the shelf zones overwhelmed by the Chinese river source, which is parallel to overall bathymetric contour in the study. The findings show that most of the sediments in the study area represent a mix of these sources, corroborating earlier findings (Um et al. 2017; Lee et al. 2019). In particular, the coastal zones are predominantly influenced by KR sources, which account for over 60% of the total contribution. This trend is especially prominent in bays directly influenced by rivers and streams, such as the Seomjin and Nakdong Rivers

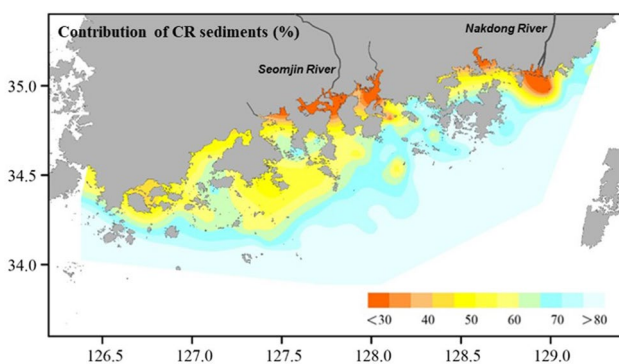


Fig. 4 Spatial variations in quantitative source apportionments of the sediments originating from Chinese rivers (CR) in the entire South Sea region, Korea. Note that CR sediments are more prevalent in the shelf area

(Fig. 4). Conversely, the shelf area is primarily composed of sediments sourced from Chinese rivers, making up 60–90% of the total volume (Fig. 4). This significant contribution from Chinese rivers to the South Sea shelf can be attributed to the considerable influx of the TWC, which carries energy (e.g., heat and moisture) and materials (e.g., nutrients and particulates) from the East China Sea to the South Sea of Korea and the YECS. This suggests an extensive offshore supply originating from the northern East China Sea shelf, where large quantities of fine-grained sediments, either from the Huanghe or Changjiang accumulated (Lim et al. 2007; Youn and Kim 2011; Hu et al. 2014b; Dou et al. 2015). Consequently, the high deposition of CR sediments in Korea's shelf regions results from the transport of reworked sediments from the East China Sea shelf along the TWC pathway, particularly during the winter season.

Meanwhile, the transport of CR sediments from the shelf regions to coastal embayment zones appears to be influenced by strong tidal currents and their asymmetry in magnitude between flood and ebb in the embayment coastal areas. Specifically, hydrodynamic observation data from the Yeosu Sound, connected to Gwangyang Bay, indicated higher concentrations of suspended sediments in the near-bottom water and a pattern of tidal asymmetry with stronger flood currents (Kim and Kang 1991). This observation implies that the amount of suspended sediments entering Gwangyang Bay through the Yeosu Sound surpasses the quantity transported out of the bay, highlighting that fine offshore and shelf sediments can be effectively transported to coastal embayment regions. Hence, the combination of stronger flood currents and higher concentration of suspended sediments near the bottom plays a crucial role in the deposition of CR sediments in the coastal embayments of the South Sea.

Another possible mechanism for the high contribution of CR sediments in the South Sea of Korea is the influence of the CWC, which branches off from the TWC and forms a robust eastward flow, circulating clockwise around Jeju Island. This current transports a substantial quantity of suspended particulate matter, estimated at approximately 23×10^6 ton year⁻¹ (Chung et al. 2000), into the South Sea. This is comparable to the total sediment loads of all Korean rivers, which range from ~ 11 to 39×10^6 ton year⁻¹, Lim et al. 2007). Recent studies have proposed that sediments reworked from the Southeastern Yellow Sea Mud (SEYSM) (Heuksan Mud Belg, HMB) deposits along the southwestern Korean coastal zone are carried into the South Sea by the CWC (Um et al. 2017; Lee et al. 2019). The SEYSM deposits, representative of offshore mud deposition in Korea, comprise multiple sediment sources (Kwak et al. 2016; Lim et al. 2020 and reference therein), including CR sediments, which contribute about 50% of the total deposition (Park et al. 2017; Lim et al. 2020). Hence, the spatial variations in sediment sources within the South Sea shelf are strongly

influenced by the TWC and/or CWC, which transport sediments originating from the Changjiang- and/or Hunanghe from the northern East China Sea shelf and/or the southern SEYSM deposits.

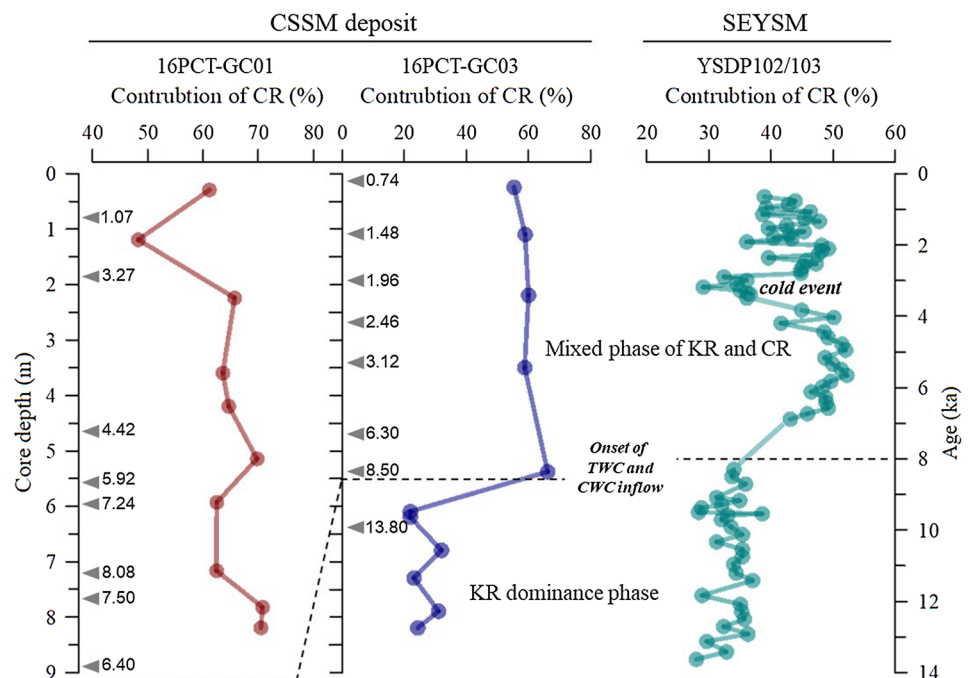
Despite potential uncertainties in our quantitative estimates, it is evident that sediment derived from CR sources plays a crucial role in forming the shelf mud deposits in the South Sea of Korea, constituting more than 60% of the total sediment budget. This finding provides a compelling explanation for the discrepancy previously noted between the volumes of KR's sediment inputs and the accumulation budget of muddy deposits in Korean coastal zones. For instance, the Nakdong and the Seomjin Rivers discharge approximately 0.8×10^6 ton year⁻¹ and $4.6\text{--}10 \times 10^6$ ton year⁻¹ of particulate matter, respectively, into the South Sea (Lim et al. 2007 and references therein). However, the sediment budgets of these Korean rivers are deemed insufficient to explain the formation of the thick mud deposits in the coastal and inner shelf regions of the South Sea (Lim et al. 2007; Bae 2015; Lee et al. 2023). Furthermore, our findings suggest that most sediments from Korean rivers are retained within coastal embayments along the shoreline, with only minimal amount being transported into the shelf region (Fig. 4).

An additional significant aspect of this study is the temporal variation in sediment sources observed in two well-dated sediment cores from the CSSM deposits developed on the inner shelf of the South Sea (Fig. 5). Similar to the surface sediments, all core sediment samples exhibit a scattered distribution between the KR and CR sediments (Fig. 2b), indicative of a mixture of both sources. The proportion of CR sediments in the cores varied between 20 and

70% over time, suggesting substantial temporal changes in sediment source-to-sink dynamics. Of particular note is the abrupt shift from KR's sediment dominance to CR sediment dominance around 8 kyr BP (Fig. 5). Prior to approximately 8–10 kyr BP, the CSSM deposits were primarily composed of KR sediments, accounting for over ~75% of total sediment budget. However, during the late-to-middle Holocene after ~8 kyr BP, there was a relatively high contribution of CR sediments (approximately 50–70%). This sudden and marked shift in the dominant sediment source is closely linked the evolution of the ocean current system in response to the incursion of the TWC, coupled with rising sea level.

The prevailing sea-level low-stand before the Holocene led to the seaward extension of the coastline and the emergence of the exposed shelf in the South Sea of Korea. In the study area, the paleo-shoreline was located approximately 60 km southeast of its present position, and rivers such as the Seomjin River stretched southward, resulting in the incision of the continental shelf (Park et al. 2000; Bae et al. 2018). Notably, sediments from the paleo-Seomjin River accumulated within the widely developed incised valleys on the modern shelf of the central South Sea (Bae et al. 2014, 2018; Lee et al. 2017). During this period, the Chinese rivers (i.e., the Huanghe and Changjiang) flowed into the edge of the East China Sea shelf near the northern Okinawa Trough (Li et al. 2015; Xu et al. 2017). Besides, it is probable that the TWC was either absent or extremely weak in the epi-continental shelf regions of the northwestern Pacific marginal seas, including the South Sea, during this time (Diekmann et al. 2008; Lim et al. 2015a; Xu et al. 2014). Consequently, the contributions from paleo-Chinese Rivers to the South

Fig. 5 Down-core variations of quantitative contribution of the CR in cores from the central South Sea mud (CSSM) and the southeastern Yellow Sea mud (SEYSM) deposits during the last 14 kyrs. Numbers in cores 16PCT-GC01 and 16PCT-GC03 indicate ages (kyr BP) of sediment layers (Age data from Lee et al. 2019). The data of cores YSDP 102 and 103 from Lim et al. (2020). Note an abrupt shift in sediment sources in both Korean coastal regions around 8 kyr BP



Sea of Korea were minimal or non-existent. Thus, the central South Sea shelf was mainly filled with the Seomjin River-sourced sediments during the sea-level low-stand before approximately 8 kyr BP, leading to a high proportion of KR sources in sediment cores.

With the rise in sea level during the Holocene, the coastline and the mouths of Korean rivers likely receded gradually, causing most of the KR sediments to be trapped within the present estuaries and coastal embayments, as evidenced by the high proportion of KR sources depicted in Fig. 4. Concurrently, the shelf environmental system was governed by oceanic currents, especially the TWC, which facilitated the extensive northward transport of CR-sourced sediments from Chinese rivers across the East China Sea shelf. In addition, the Changjiang Diluted Water plume (Fig. 1a) contributed to the northeastward movement of some Changjiang sediments, particularly during intense monsoon seasons. Therefore, the sudden increase in the CR source contribution since around 8 kyr BP could be attributed to the intrusion of the TWC into the study area. Moreover, this temporal shift in sediment sources coincides with the notion that the postglacial sea-level rise was nearly completed by around 8 kyr BP, at which point the modern oceanic circulation patterns were established. Studies examining the development of the TWC, particularly in the Korean Strait and the Hupo Basin of the southeastern Korean shelf, support our interpretation that the TWC likely stabilized at this time and flowed into the East/Japan Sea through this strait (Lim et al. 2006b; Khim et al. 2021).

This historical progression of sedimentation and the ocean current system is evident in sediment core (YSDP 102 and 103, refer to Fig. 1b for core sites) from the southern part of the SEYSM deposit along the southwestern coasts of Korea. As indicated in Fig. 5, in these cores, the contribution of CR sediments also increased significantly since around 8 kyr BP, which demonstrate a tentative correlation between the sediment source variation and the onset of Yellow Sea Warm Current (YSWC) inflow into the Yellow Sea (Lim et al. 2020). In the Yellow Sea at this time, the dominant sediment source remarkably changed to the Changjiang, while the supplies from Huanghe decreased (Lim et al. 2015a). This noticeable change is also associated with the formation of the modern surface water circulation system with the dominance of the YSWC and the Yellow Sea coastal current (YSCC) mainly controlled riverine supply to the CYSM, while the importance of estuary shift, tidal stress, sea-level fluctuation, and monsoon climate change was significantly weakened. With respect to its relevance to historical sedimentary deposits of the YECS sediments over the last approximately 14 kyr BP (Fig. 5), our fingerprint-inferred provenance changes depict a distinct sedimentation trend over the course of the Holocene, marked by a substantial increase in the CR contribution since around 8 kyr BP.

Nonetheless, determining the precise onset timing of ocean circulation systems and their final formation coupled with sea level rise in the northern Pacific marginal seas (i.e., the Yellow Sea, South Sea of Korea, and East/Japan Sea) necessitates further investigation through the comprehensive correlation of well-dated sediment cores.

As shown in the core 16PCT-GC03 (Fig. 5), besides, the sedimentation rate in the shelf region significantly increased from ~ 0.37 m/ka during the middle Holocene (~ 8.5 to ~ 3.12 ka) to ~ 1.12 m/ka since ~ 3 ka. This increase is also evident in another sediment core (SSDP103) from the CSSM deposit: in this sediment core, the sedimentation rate is low at ~ 2.47 m/ka in the middle Holocene, but increased more than five times (~ 10.20 m/ka) during the late Holocene (data from Kong et al. 2013). The results suggest that sediments originating from the East China Sea and/or the southwestern Korean coastal zone were deposited at much higher sedimentation rates as sea level rise slowed or stabilized during the late Holocene. The relatively high sediment deposition during the late Holocene may be linked to strengthened YSWC and CWC since ~ 4 ka (Kong et al. 2006; Li et al. 2009), leading to enhanced sediment supply from the northern East China Sea (e.g., ECSDM) and the SEYSM; however, temporal changes in the sedimentation rates and sediment sources in the sediment cores from additional locations will be necessary for better defining the long-term depositional mechanism in the shelf zone of the South Sea.

5 Conclusions

In this study, we analyzed a comprehensive dataset that encompasses the Al and Mg contents from surface sediment samples and two sediment cores, integrating previously reported data. Objective of this study was to scrutinize the spatial and temporal variations in the sources of these sediments throughout the entire South Sea region, inclusive of the coastal and shelf zones. To quantitatively estimate the sediment sources, we used the Al–Mg regression model, which unearthed notable spatial variations in the contributions from Korean and Chinese rivers. In the coastal zone of the South Sea, KR sediments constitute over 60–70% of the total; however, this proportion drops to 10–20% in the shelf zone. This finding signifies that most of the sediments from Korean rivers are confined within the coastal embayments along the shoreline, with only a scant amount extending into the shelf region. In contrast, the shelf regions of the South Sea are predominantly blanketed by fine-grained sediments that originate from Chinese rivers, accounting for over 70% of the total sediment budget. This underscores the significant influence of CR sediments on the formation of muddy deposits in the central South Sea, lending credence to the

multi-source concept for the CSSM. Besides, our results delineate a distinct sedimentation trend over the course of the Holocene period, characterized by a substantial increase in the contribution of CR sediments commencing around 8 kyr BP. This depositional history of shelf mud deposits is intimately connected to the evolution of the TWC inflow. By quantifying and elucidating the sediment sources throughout the South Sea, this research enhances our understanding of the sediment routing system and depositional evolution of mud depositions in the marginal sea with large rivers, such as the Huanhge and the Changjiang.

Acknowledgements This work was supported by National Research Foundation of Korea (grant no. NRF-2022R1A2C1006208) and Korea Institute of Marine Science & Technology (KIMST) funded by the Ministry of Oceans and Fisheries (RS-2023-00256330, Development of risk managing technology tackling ocean and fisheries crisis around Korean Peninsula by Kuroshio Current). We thank the Library of Marine Sample (LIMS), Korea Institute of Ocean Science and Technology (KIOST) for supplying the samples.

Data availability The original contributions presented in the study are given in the article.

References

- Allen PA (2017) Sediment routing systems: the fate of sediment from source to sink. Cambridge University Press, London, p 422
- Bae SH (2015) Depositional environment of the late Quaternary deposit in the southern and southwestern inner shelf of Korea. Ph.D. thesis, Pukyong National University, p 195
- Bae SH, Kim DC, Lee GS, Kim GY, Kim SP, Seo YK, Kim JC (2014) Physical and acoustic properties of inner shelf sediments in the South Sea, Korea. *Quat Int* 344:125–142. <https://doi.org/10.1016/j.quaint.2014.03.058>
- Bae SH, Kong GS, Lee GS, Yoo DG (2018) Incised channel morphology and depositional fill of the paleo-Seomjin River in the continental shelf of the South Sea, Korea. *Quat Int* 468:49–61. <https://doi.org/10.1016/j.quaint.2017.03.053>
- Bian CW, Jiang WS, Greatbatch RJ (2013) An exploratory model study of sediment transport sources and deposits in the Bohai Sea, Yellow Sea, and East China Sea. *J Geophys Res Oceans* 118:5908–5923. <https://doi.org/10.1002/2013JC009116>
- Cho YG (1994) Distribution and origin of metallic elements in marine sediments around Korean Peninsula. Ph.D. thesis, Seoul National University, p 261
- Cho YG, Lee CB, Choi MS (1999) Geochemistry of surface sediments off the southern and western coast of Korea. *Mar Geol* 159:111–129. [https://doi.org/10.1016/S0025-3227\(98\)00194-7](https://doi.org/10.1016/S0025-3227(98)00194-7)
- Cho HG, Kim SO, Kwak KY, Choi HS, Kim BK (2015) Clay mineral distribution and provenance in the Heuksan mud belt, Yellow Sea. *Geo-Mar Lett* 35:411–419. <https://doi.org/10.1007/s00367-015-0417-3>
- Chough SK, Lee HJ, Yoon SH (2000) Marine geology of Korean seas. Elsevier, Amsterdam, p 313
- Chung CS, Hong GH, Kim SH, Park JK, Kim YI, Moon DS, Chang KI, Nam SY, Park YC (2000) Biochemical fluxes through the Cheju Strait. *Sea J Korean Soc Oceanogr* 5:208–215
- Diekmann B, Hofmann J, Henrich R, Fütterer DK, Röhl U, Wei KY (2008) Detrital sediment supply in the southern Okinawa Trough and its relation to sea-level and Kuroshio dynamics during the late Quaternary. *Mar Geol* 255:83–95. <https://doi.org/10.1016/j.margeo.2008.08.001>
- Dou YG, Yang SY, Lim DI, Jung HS (2015) Provenance discrimination of last deglacial and Holocene sediments in the southwest of Cheju Island, East China Sea. *Palaeogeogr Palaeoclimatol* 422:25–35. <https://doi.org/10.1016/j.palaeo.2015.01.016>
- Dou YG, Yang SY, Shi XF, Clift PD, Liu SF, Liu J, Li C (2016) Provenance weathering and erosion records in southern Okinawa Trough sediments since 28 ka: geochemical and Sr–Nd–Pb isotopic evidences. *Chem Geol* 425:93–109. <https://doi.org/10.1016/j.chemgeo.2016.01.029>
- Hsiung KH, Saito Y (2017) Sediment trapping in deltas of small mountainous rivers of southwestern Taiwan and its influence on East China Sea. *Quat Int* 455:30–44. <https://doi.org/10.1016/j.quaint.2017.02.020>
- Hu DX (1984) Upwelling and sedimentation dynamics. *Chin J Oceanol Limnol* 2:12–19. <https://doi.org/10.1007/BF02888388>
- Hu Q, Li J, Zhao J, Yan H, Zou L, Bai F, Xu F, Yin X, Wei G (2014a) Sr–Nd isotopic geochemistry of Holocene sediments from the South Yellow Sea: implications for provenance and monsoon variability. *Chem Geol* 479:102–112. <https://doi.org/10.1016/j.chemgeo.2017.12.033>
- Hu Q, Yang ZS, Qiao SQ, Zhao MX, Fan DJ, Wang HJ, Bi NS, Li J (2014b) Holocene shifts in riverine fine-grained sediment supply to the East China Sea Distal Mud in response to climate change. *Holocene* 24:1253–1268. <https://doi.org/10.1177/0959683614540>
- Ingram RL (1971) Sieve analysis. In: Carver RE (ed) Procedures in sedimentary petrology. Wiley-Interscience, New York, pp 49–67
- Jung HS, Kim JH, Lim D, Jeong D, Lee J, Xu Z (2021) REE fractionation and quantification of sediment source in the Yellow Sea mud deposits, East Asian marginal sea. *Cont Self Sci* 217:104374. <https://doi.org/10.1016/j.csr.2021.104374>
- Khim BK, Kim S, Park YH, Lee J, Ha S, Yoo KC (2021) Holocene sedimentation in the Hupo Trough of the southwestern East Sea (Japan Sea) and development of the East Korea Warm Current. *Holocene* 31:1148–1157. <https://doi.org/10.1177/09596836211003238>
- Kim DC, Kang HJ (1991) Suspended sediment budget in Gwangyang Bay through the Yeosu Sound. *Bull Korean Fish Soc* 24:31–38
- Kim GY, Park KJ, Lee GS, Yoo DG, Kong GS (2019) Physical property characterization of quaternary sediments in the vicinity of the paleo-Seomjin River of the continental shelf of the South Sea, Korea. *Quat Int* 503:153–162. <https://doi.org/10.1016/j.quaint.2018.09.002>
- Kong GS, Park SC, Han HC, Chang JH, Mackensen A (2006) Late Quaternary paleoenvironmental changes in the southeastern Yellow Sea, Korea. *Quat Int* 144:38–52. <https://doi.org/10.1016/j.quaint.2005.05.011>
- Kong GS, Kim K-O, Kim S-P (2013) Characteristics of the East Asian summer monsoon in the South Sea of Korea during the Little Ice Age. *Quat Int* 286:36–44. <https://doi.org/10.1016/j.quaint.2012.07.022>
- Koo HJ, Cho HG (2020) Changes in detrital sediment supply to the central Yellow Sea since the last deglaciation. *Ocean Sci* 16:1247–1259. <https://doi.org/10.5194/os-16-1247-2020>
- Koo H, Lee Y, Kim S, Cho H (2018) Clay mineral distribution and provenance in surface sediments of Central Yellow Sea Mud. *Geosci J* 22:989–1000. <https://doi.org/10.1007/s12303-018-0019-y>
- Kwak K, Choi H, Cho HG (2016) Paleo-environmental change during the late Holocene in the southeastern Yellow Sea, Korea. *Appl Clay Sci* 134:55–61. <https://doi.org/10.1016/j.clay.2016.05.007>
- Lee GS, Cuker D, Yoo DG, Bae SH, Kong GS (2017) Sequence stratigraphy and evolution history of the continental shelf of South

- Sea, Korea, since the Last Glacial Maximum (LGM). *Quat Int* 459:17–28. <https://doi.org/10.1016/j.quaint.2017.09.002>
- Lee HG, Park WY, Koo HG, Choi JY, Jang JK, Cho HG (2019) Changes in provenance and transport process of fine sediments in central South Sea mud. *J Miner Soc Korea* 32:235–247
- Lee B, Yoo D, Lim D (2023) Source-to-sink system (S2S) of the shelf mud deposits on the Korean continental shelf. In: Abstracts of the Korean Society of Oceanography symposium, BEXCO, Pusan, 2–4 May 2023
- Li TG, Nan QY, Jiang B, Sun RT, Zhang DY, Li Q (2009) Formation and evolution of the modern warm current system in the East China Sea and the Yellow Sea since the last deglaciation. *Chin J Oceanol Limn* 27:237–249. <https://doi.org/10.1007/s00343-009-9149-4>
- Li J, Hu BQ, Wei HL, Zhao JT, Zou L, Bai FL, Dou YG, Wang LB, Fang XS (2014) Provenance variations in the Holocene deposits from the southern Yellow Sea: clay mineralogy evidence. *Cont Shelf Res* 90:41–51. <https://doi.org/10.1016/j.csr.2014.05.001>
- Li T, Xu Z, Lim D, Chang F, Wan S, Jung H, Choi J (2015) Sr–Nd isotopic constraints on detrital sediment provenance and paleoenvironmental change in the northern Okinawa trough during the late Quaternary. *Palaeogeogr Palaeoclimatol* 430:74–84. <https://doi.org/10.1016/j.palaeo.2015.04.017>
- Lim D, Jung HS, Choi JY, Yang S, Ahn KS (2006a) Geochemical compositions of river and shelf sediments in the Yellow Sea: grain-size normalization and sediment provenance. *Cont Shelf Res* 26:15–24. <https://doi.org/10.1016/j.csr.2005.10.001>
- Lim D, Kang S, Yoo HS, Jung HS, Choi JY, Kim HN, Shin IH (2006b) Late Quaternary sediments on the outer shelf of the Korea Strait and their paleoceanographic implications. *Geo-Mar Lett* 26:287–296. <https://doi.org/10.1007/s00367-006-0039-x>
- Lim D, Choi JY, Jung HS, Rho KC, Ahn KS (2007) Recent sediment accumulation and origin of shelf mud deposits in the Yellow and East China Seas. *Prog Oceanogr* 73:145–159. <https://doi.org/10.1016/j.pocean.2007.02.004>
- Lim D, Choi JY, Shin HH, Rho KC, Jung HS (2013) Multielement geochemistry of offshore sediment origin and dispersal. *Quat Int* 298:196–206. <https://doi.org/10.1016/j.quaint.2013.01.004>
- Lim D, Jung HS, Choi JY (2014) REE partitioning in riverine sediments around the Yellow Sea and its importance in shelf sediment provenance. *Mar Geol* 357:12–24. <https://doi.org/10.1016/j.margeo.2014.07.002>
- Lim D, Xu Z, Choi JY, Li T, Kim SY (2015a) Holocene changes in detrital sediment supply to the eastern part of the Central Yellow Sea and their forcing mechanisms. *J Asian Earth Sci* 105:18–31. <https://doi.org/10.1016/j.jseaes.2015.03.032>
- Lim D, Jung HS, Xu Z, Jeong KS, Li T (2015b) Elemental and Sr–Nd isotopic compositional disparity of riverine sediments around the Yellow Sea: constraints from grain-size and chemical partitioning. *Appl Geochem* 63:272–281. <https://doi.org/10.1016/j.apgeochem.2015.09.018>
- Lim D, Kim J, Xu Z, Jung H, Yoo D, Choi M, Kim S (2020) Quantitative reconstruction of Holocene sediment source variations in the Yellow and northern East China Seas and their forcings. *Mar Geol* 430:106345. <https://doi.org/10.1016/j.margeo.2020.106345>
- Milliman JD, Meade RH (1983) World-wide delivery of river sediment to the oceans. *J Geol* 91:1–21
- Nam HL (2016) Geochemical behavior characteristics and environment impact assessment of surface sediments in mid to downstream of the Seomjin River. MS thesis, Chonnam National University, p 48
- Park Y, Khim BK (1992) Origin and dispersal of recent clay minerals in the Yellow Sea. *Mar Geol* 104:205–213. [https://doi.org/10.1016/0025-3227\(92\)90095-y](https://doi.org/10.1016/0025-3227(92)90095-y)
- Park SC, Hong SK, Kim DC (1996) Evolution of late Quaternary deposits on the inner shelf of the South Sea of Korea. *Mar Geol* 131:219–232. [https://doi.org/10.1016/0025-3227\(96\)00006-0](https://doi.org/10.1016/0025-3227(96)00006-0)
- Park SC, Lee HH, Han HS, Lee GH, Kim DC, Yoo DG (2000) Evolution of late Quaternary mud deposits and recent sediment budget in the southeastern Yellow Sea. *Mar Geol* 170:271–288. [https://doi.org/10.1016/S0025-3227\(00\)00099-2](https://doi.org/10.1016/S0025-3227(00)00099-2)
- Park JK, Choi MS, Song Y, Lim D (2017) Tracing the Origin of Pb using Stable Pb Isotopes in Surface Sediments along the Korean Yellow Sea Coast. *Ocean Sci J* 52:177–192. <https://doi.org/10.1007/s12601-017-0020-9>
- Shi XF, Shen SX, Yi HL, Chen ZH, Meng Y (2003) Modern sedimentary environments and dynamic depositional systems in the southern Yellow Sea. *Chin Sci Bull* 48:1–7. <https://doi.org/10.1007/BF02900933>
- Um IK, Choi MS, Lee GS, Chang TS (2015) Origin and depositional environment of fine-grained sediments since the last glacial maximum in the southeastern Yellow Sea: evidence from rare earth elements. *Geo-Mar Lett* 35:421–431. <https://doi.org/10.1007/s00367-015-0416-4>
- Um IK, Choi MS, Bae SH, Song YH, Kong GS (2017) Provenance of fine-grained sediments in the inner shelf of the Korea Strait (South Sea), Korea. *Ocean Sci J* 53:31–42. <https://doi.org/10.1007/s12601-017-0062-z>
- Wang YH, Li GX, Zhang WG, Dong P (2014) Sedimentary environment and formation mechanism of the mud deposit in the central South Yellow Sea during the past 40 kyr. *Mar Geol* 347:123–135. <https://doi.org/10.1016/j.margeo.2013.11.008>
- Wang JZ, Li AC, Xu KH, Zheng XF, Huang J (2015) Clay mineral and grain size studies of sediment provenances and paleoenvironment evolution in the middle Okinawa Trough since 17 ka. *Mar Geol* 366:49–61. <https://doi.org/10.1016/j.margeo.2015.04.007>
- Xu ZK, Lim D, Choi JY, Yang SY, Jung HS (2009) Rare earth elements in bottom sediments of major rivers around the Yellow Sea: implications for sediment provenance. *Geo-Mar Lett* 29:291–300. <https://doi.org/10.1007/s00367-009-0142-x>
- Xu ZK, Li TG, Chang FM, Wan SM, Choi JY, Lim DI (2014) Clay-sized sediment provenance change in the northern Okinawa Trough since 22 kyr BP and its paleoenvironmental implication. *Palaeogeogr Palaeoclimatol* 399:236–245. <https://doi.org/10.1016/j.palaeo.2014.01.016>
- Xu ZK, Li T, Clift PD, Lim D, Nan Q, Wan S, Choi J, Cai M, Chen H (2017) Sediment provenance and paleoenvironmental change in the middle Okinawa Trough during the last 18.5 kyr: clay mineral and geochemical evidence. *Quat Int* 440:139–149. <https://doi.org/10.1016/j.quaint.2016.07.058>
- Yang SY, Youn JS (2007) Geochemical compositions and provenance discrimination of the central Yellow Sea sediment. *Mar Geol* 243:229–241. <https://doi.org/10.1016/j.margeo.2007.05.001>
- Yang SY, Jung HS, Lim DI, Li CX (2003) A review on the provenance discrimination of sediments in the Yellow Sea. *Earth Sci Rev* 63:93–120. [https://doi.org/10.1016/S0012-8252\(03\)00033-3](https://doi.org/10.1016/S0012-8252(03)00033-3)
- Yoo DG, Lee GS, Kim GY, Kang NK, Yi BY, Kim YJ, Chun JH, Kong GS (2016) Seismic stratigraphy and depositional history of late Quaternary deposits in a tide dominated setting: an example from the eastern Yellow Sea. *Mar Pet Geol* 73:212–227. <https://doi.org/10.1016/j.marpetgeo.2016.03.005>
- Youn J, Kim TJ (2011) Geochemical composition and provenance of muddy shelf deposits in the East China Sea. *Quat Int* 230:3–12. <https://doi.org/10.1016/j.quaint.2009.11.001>
- Zhao DB, Wan SM, Clift PD, Tada R, Huang J, Yin XB, Liao RQ, Shen XY, Shi XF, Li AC (2018) Provenance, sea-level and

monsoon climate controls on silicate weathering of Yellow River sediment in the northern Okinawa Trough during late last glaciation. *Palaeogeogr Palaeoclimatol* 490:227–239. <https://doi.org/10.1016/j.palaeo.2017.11.002>

Publisher's Note Springer Nature remains neutral with regard to jurisdictional claims in published maps and institutional affiliations.

Springer Nature or its licensor (e.g. a society or other partner) holds exclusive rights to this article under a publishing agreement with the author(s) or other rightsholder(s); author self-archiving of the accepted manuscript version of this article is solely governed by the terms of such publishing agreement and applicable law.